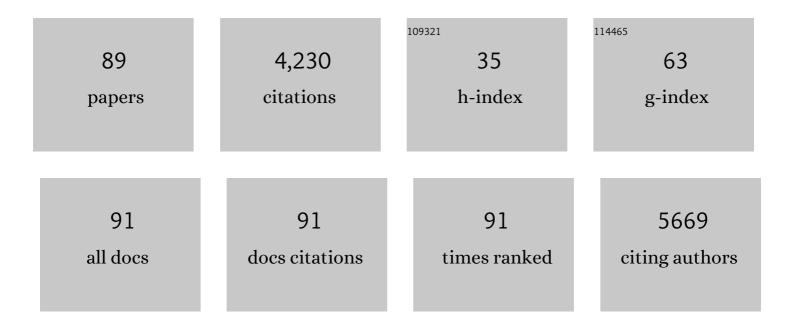
Junfeng Lu

List of Publications by Year in descending order

Source: https://exaly.com/author-pdf/697817/publications.pdf Version: 2024-02-01



LUNFENC LU

#	Article	IF	CITATIONS
1	Tripleâ€Mode Emission of Carbon Dots: Applications for Advanced Anti ounterfeiting. Angewandte Chemie - International Edition, 2016, 55, 7231-7235.	13.8	625
2	Tripleâ€Mode Emission of Carbon Dots: Applications for Advanced Anti ounterfeiting. Angewandte Chemie, 2016, 128, 7347-7351.	2.0	467
3	Improved UV photoresponse of ZnO nanorod arrays by resonant coupling with surface plasmons of Al nanoparticles. Nanoscale, 2015, 7, 3396-3403.	5.6	157
4	Achieving high-resolution pressure mapping via flexible GaN/ ZnO nanowire LEDs array by piezo-phototronic effect. Nano Energy, 2019, 58, 633-640.	16.0	120
5	Comparative investigation on temperature-dependent photoluminescence of CH ₃ NH ₃ PbBr ₃ and CH(NH ₂) ₂ PbBr ₃ microstructures. Journal of Materials Chemistry C, 2016, 4, 4408-4413.	5.5	109
6	Size Effects of Raman and Photoluminescence Spectra of CdS Nanobelts. Journal of Physical Chemistry C, 2013, 117, 20998-21005.	3.1	105
7	Facile synthesis of highly conductive sulfur-doped reduced graphene oxide sheets. Physical Chemistry Chemical Physics, 2016, 18, 1125-1130.	2.8	103
8	Large and Ultrastable Allâ€Inorganic CsPbBr ₃ Monocrystalline Films: Lowâ€Temperature Growth and Application for Highâ€Performance Photodetectors. Advanced Materials, 2018, 30, e1802110.	21.0	94
9	Nanoplate-Built ZnO Hollow Microspheres Decorated with Gold Nanoparticles and Their Enhanced Photocatalytic and Gas-Sensing Properties. ACS Applied Materials & Interfaces, 2015, 7, 11824-11832.	8.0	89
10	Aeolian desertification and its causes in the Zoige Plateau of China's Qinghai–Tibetan Plateau. Environmental Earth Sciences, 2010, 59, 1731-1740.	2.7	88
11	Highâ€Altitude Aeolian Research on the Tibetan Plateau. Reviews of Geophysics, 2017, 55, 864-901.	23.0	87
12	Piezoelectricity in Multilayer Black Phosphorus for Piezotronics and Nanogenerators. Advanced Materials, 2020, 32, e1905795.	21.0	84
13	Single Mode ZnO Whispering-Gallery Submicron Cavity and Graphene Improved Lasing Performance. ACS Nano, 2015, 9, 6794-6800.	14.6	78
14	Controllable Growth of Aligned Monocrystalline CsPbBr ₃ Microwire Arrays for Piezoelectricâ€Induced Dynamic Modulation of Singleâ€Mode Lasing. Advanced Materials, 2019, 31, e1900647.	21.0	76
15	Template-free synthesis of porous ZnO/Ag microspheres as recyclable and ultra-sensitive SERS substrates. Applied Surface Science, 2018, 427, 830-836.	6.1	74
16	Self-powered high-performance flexible GaN/ZnO heterostructure UV photodetectors with piezo-phototronic effect enhanced photoresponse. Nano Energy, 2022, 94, 106945.	16.0	73
17	Self-assembled ZnO/Ag hollow spheres for effective photocatalysis and bacteriostasis. Materials Research Bulletin, 2018, 98, 64-69.	5.2	71
18	Direct Resonant Coupling of Al Surface Plasmon for Ultraviolet Photoluminescence Enhancement of ZnO Microrods. ACS Applied Materials & Interfaces, 2014, 6, 18301-18305.	8.0	69

JUNFENG LU

#	Article	IF	CITATIONS
19	Progress in piezotronic and piezo-phototronic effect of 2D materials. 2D Materials, 2018, 5, 042003.	4.4	62
20	Plasmon-enhanced ZnO whispering-gallery mode lasing. Nano Research, 2018, 11, 3050-3064.	10.4	61
21	Reversible Conversion between Schottky and Ohmic Contacts for Highly Sensitive, Multifunctional Biosensors. Advanced Functional Materials, 2020, 30, 1907999.	14.9	61
22	Crystal structure and electron transition underlying photoluminescence of methylammonium lead bromide perovskites. Journal of Materials Chemistry C, 2017, 5, 7739-7745.	5.5	58
23	Triboelectric Nanogenerator Enhanced Schottky Nanowire Sensor for Highly Sensitive Ethanol Detection. Nano Letters, 2020, 20, 4968-4974.	9.1	58
24	Dynamically Modulated GaN Whispering Gallery Lasing Mode for Strain Sensor. Advanced Functional Materials, 2019, 29, 1905051.	14.9	56
25	Plasmon-Enhanced Whispering Gallery Mode Lasing from Hexagonal Al/ZnO Microcavity. ACS Photonics, 2015, 2, 73-77.	6.6	54
26	Lasing mode regulation and single-mode realization in ZnO whispering gallery microcavities by the Vernier effect. Nanoscale, 2016, 8, 16631-16639.	5.6	54
27	Piezoelectric Effect Tuning on ZnO Microwire Whispering-Gallery Mode Lasing. ACS Nano, 2018, 12, 11899-11906.	14.6	51
28	Burstein-Moss Effect Behind Au Surface Plasmon Enhanced Intrinsic Emission of ZnO Microdisks. Scientific Reports, 2016, 6, 36194.	3.3	48
29	3D Ag/ZnO hybrids for sensitive surface-enhanced Raman scattering detection. Applied Surface Science, 2016, 365, 291-295.	6.1	46
30	Plasmon-enhanced Electrically Light-emitting from ZnO Nanorod Arrays/p-GaN Heterostructure Devices. Scientific Reports, 2016, 6, 25645.	3.3	42
31	Extra green light induced ZnO ultraviolet lasing enhancement assisted by Au surface plasmons. Nanoscale, 2018, 10, 623-627.	5.6	41
32	SERS-active ZnO/Ag hybrid WGM microcavity for ultrasensitive dopamine detection. Applied Physics Letters, 2016, 109, .	3.3	40
33	Plasmon-Induced Accelerated Exciton Recombination Dynamics in ZnO/Ag Hybrid Nanolasers. ACS Photonics, 2017, 4, 2419-2424.	6.6	38
34	Synthesis and investigation of blue and green emissions of ZnS ceramics. Journal of Luminescence, 2013, 134, 498-503.	3.1	37
35	Plasmon coupled Fabry-Perot lasing enhancement in graphene/ZnO hybrid microcavity. Scientific Reports, 2015, 5, 9263.	3.3	36
36	Ultrabroadband, Large Sensitivity Position Sensitivity Detector Based on a Bi ₂ Te _{2.7} Se _{0.3} /Si Heterojunction and Its Performance Improvement by Pyroâ€Phototronic Effect. Advanced Electronic Materials, 2019, 5, 1900786.	5.1	33

Junfeng Lu

#	Article	IF	CITATIONS
37	Controlled fabrication, lasing behavior and excitonic recombination dynamics in single crystal CH3NH3PbBr3 perovskite cuboids. Science Bulletin, 2019, 64, 698-704.	9.0	33
38	In ₂ O ₃ Nanowire Field-Effect Transistors with Sub-60 mV/dec Subthreshold Swing Stemming from Negative Capacitance and Their Logic Applications. ACS Nano, 2018, 12, 9608-9616.	14.6	32
39	Dynamic regulating of single-mode lasing in ZnO microcavity by piezoelectric effect. Materials Today, 2019, 24, 33-40.	14.2	32
40	Driving forces responsible for aeolian desertification in the source region of the Yangtze River from 1975 to 2005. Environmental Earth Sciences, 2012, 66, 257-263.	2.7	30
41	Equations for the nearâ€surface mass flux density profile of windâ€blown sediments. Earth Surface Processes and Landforms, 2011, 36, 1292-1299.	2.5	29
42	Phase controlled synthesis and optical properties of ZnS thin films by pulsed laser deposition. Materials Research Bulletin, 2013, 48, 3843-3846.	5.2	29
43	Driving forces of aeolian desertification in the source region of the Yellow River: 1975–2005. Environmental Earth Sciences, 2013, 70, 3245-3254.	2.7	28
44	A ZnO micro/nanowire-based photonic synapse with piezo-phototronic modulation. Nano Energy, 2021, 89, 106282.	16.0	26
45	Plasmon enhancement for Vernier coupled single-mode lasing from ZnO/Pt hybrid microcavities. Nano Research, 2017, 10, 3447-3456.	10.4	25
46	Single-mode lasing of CsPbBr ₃ perovskite NWs enabled by the Vernier effect. Nanoscale, 2021, 13, 4432-4438.	5.6	25
47	The significance of Gobi desert surfaces for dust emissions in China: an experimental study. Environmental Earth Sciences, 2011, 64, 1039-1050.	2.7	23
48	Synergistic graphene/aluminum surface plasmon coupling for zinc oxide lasing improvement. Nano Research, 2017, 10, 1996-2004.	10.4	23
49	The excitonic photoluminescence mechanism and lasing action in band-gap-tunable CdS _{1â^'x} Se _x nanostructures. Nanoscale, 2016, 8, 804-811.	5.6	22
50	Improved Whispering-Gallery Mode Lasing of ZnO Microtubes Assisted by the Localized Surface Plasmon Resonance of Au Nanoparticles. Science of Advanced Materials, 2015, 7, 1156-1162.	0.7	22
51	Tunable blue and orange emissions of ZnS:Mn thin films deposited on GaN substrates by pulsed laser deposition. Journal of Luminescence, 2014, 147, 310-315.	3.1	21
52	Spatial variability of vegetation characteristics, soil properties and their relationships in and around China's Badain Jaran Desert. Environmental Earth Sciences, 2015, 74, 6847-6858.	2.7	21
53	Crystal-Orientation-Related Dynamic Tuning of the Lasing Spectra of CdS Nanobelts by Piezoelectric Polarization. ACS Nano, 2019, 13, 5049-5057.	14.6	21
54	Mean airflow patterns upwind of topographic obstacles and their implications for the formation of echo dunes: A wind tunnel simulation of the effects of windward slope. Journal of Geophysical Research, 2011, 116, .	3.3	19

JUNFENG LU

#	Article	IF	CITATIONS
55	Preparation and Photoluminescence of (3C-ZnS)/(2H-ZnS) Superlattice in Mn-doped ZnS Nanoribbons. Journal of Physical Chemistry C, 2012, 116, 23013-23018.	3.1	19
56	The effect of desertification on carbon and nitrogen status in the northeastern margin of the Qinghai-Tibetan Plateau. Environmental Earth Sciences, 2014, 71, 807-815.	2.7	19
57	Controlled growth and photoluminescence of one-dimensional and platelike ZnS nanostructures. Applied Surface Science, 2012, 258, 8538-8541.	6.1	17
58	Grain-size characteristics of linear dunes on the northern margin of Qarhan Salt Lake, northwestern China. Journal of Arid Land, 2015, 7, 438-449.	2.3	16
59	Functional group dominance and not productivity drives species richness. Plant Ecology and Diversity, 2016, 9, 141-150.	2.4	16
60	Geomorphology of star dunes in the southern Kumtagh Desert, China: control factors and formation. Environmental Earth Sciences, 2013, 69, 267-277.	2.7	15
61	Magnitude of Species Diversity Effect on Aboveground Plant Biomass Increases Through Successional Time of Abandoned Farmlands on the Eastern Tibetan Plateau of China. Land Degradation and Development, 2017, 28, 370-378.	3.9	15
62	Aeolian transport over a developing transverse dune. Journal of Arid Land, 2014, 6, 243-254.	2.3	14
63	Tailored Fabrication of <i>α</i> -Fe ₂ O ₃ Nanocrystals/Reduced Graphene Oxide Nanocomposites with Excellent Electromagnetic Absorption Property. Journal of Nanoscience and Nanotechnology, 2016, 16, 12590-12601.	0.9	14
64	Pattern analysis of a linear dune field on the northern margin of Qarhan Salt Lake, northwestern China. Journal of Arid Land, 2016, 8, 670-680.	2.3	14
65	Green emission and Ag ⁺ sensing of hydroxy double salt supported gold nanoclusters. Nanoscale, 2016, 8, 5120-5125.	5.6	14
66	Plasmon-mediated exciton–phonon coupling in a ZnO microtower cavity. Journal of Materials Chemistry C, 2016, 4, 7718-7723.	5.5	13
67	Optical performance improvement in hydrothermal ZnO/graphene structures for ultraviolet lasing. Journal of Materials Chemistry C, 2018, 6, 3240-3244.	5.5	13
68	Influence of the gap ratio on variations in the surface shear stress and on sand accumulation in the lee of two side-by-side obstacles. Environmental Earth Sciences, 2016, 75, 1.	2.7	11
69	Dual-band Fabry-Perot lasing from single ZnO microbelt. Optical Materials, 2016, 60, 366-372.	3.6	11
70	Wavelength tunable single-mode lasing from cesium lead halide perovskite microwires. Applied Physics Letters, 2021, 118, .	3.3	11
71	Underlying mechanism of blue emission enhancement in Au decorated p-GaN film. RSC Advances, 2017, 7, 15071-15076.	3.6	10
72	Rücktitelbild: Tripleâ€Mode Emission of Carbon Dots: Applications for Advanced Anti ounterfeiting (Angew. Chem. 25/2016). Angewandte Chemie, 2016, 128, 7384-7384.	2.0	9

Junfeng Lu

#	Article	IF	CITATIONS
73	Two Photon–Pumped Whisperingâ€Gallery Mode Lasing and Dynamic Regulation. Advanced Science, 2019, 6, 1900916.	11.2	9
74	Optical and Exciton Dynamical Properties of a Screw-Dislocation-Driven ZnO:Sn Microstructure. ACS Applied Materials & amp; Interfaces, 2015, 7, 12655-12662.	8.0	8
75	Interconnected SnO2 Microsphere Films with Improved Ultraviolet Photodetector Properties. Journal of Electronic Materials, 2017, 46, 6669-6676.	2.2	8
76	Energy band modification for UV photoresponse improvement in a ZnO microrod-quantum dot structure. RSC Advances, 2016, 6, 687-691.	3.6	7
77	Tunable single-mode lasing in a single semiconductor microrod. Optics Express, 2018, 26, 30021.	3.4	6
78	Effects of Au catalysts for synthesis of ZnS microstructures on the sapphire substrate. Materials Letters, 2013, 93, 337-340.	2.6	5
79	Brightness improvement in a graphene inserted GaN/ZnO heterojunction light emitting diode. Journal Physics D: Applied Physics, 2019, 52, 395104.	2.8	4
80	Thermal effect induced dynamically lasing mode tuning in GaN whispering gallery microcavities. Journal Physics D: Applied Physics, 2021, 54, 255103.	2.8	4
81	Dynamic regulating of lasing mode in a whispering-gallery microresonator by thermo-optic effect. Applied Physics Letters, 2021, 119, .	3.3	4
82	Photoelectric dual-mode strain sensing based on piezoelectric effect. Journal of Luminescence, 2021, 238, 118237.	3.1	4
83	Lasing behavior modulation in a layered cylindrical microcavity. Applied Physics B: Lasers and Optics, 2015, 118, 93-100.	2.2	3
84	Optical Field Confinement Enhanced Single ZnO Microrod UV Photodetector. Chinese Physics Letters, 2017, 34, 078503.	3.3	3
85	Realizing single-mode lasing in all-inorganic CsPbBr3 perovskite microwires using intrinsic self-absorption. Applied Physics Letters, 2022, 120, .	3.3	2
86	Monitoring land use and land cover change in the source region of the Yangtze River using multi-temporal Landsat data. , 2011, , .		1
87	Strain-modulated high-quality ZnO cavity modes on different crystal orientations. Nanotechnology, 2020, 31, 225202.	2.6	0
88	Graphene induced lasing mode tailoring in GaN floating microring cavity. Europhysics Letters, 0, , .	2.0	0
89	10.1063/5.0062761.1., 2021, , .		0